Distribution Category:
Magnetic Fusion Energy-
Fusion Systems (UC-20d)

ANL/FPP/TM-214

ANL/FPP/TM--214

DE88 003973

Argonne National Laboratory
9700 South Cass Avenue
Argonne, Illinois 60439

APPLICATION OF HIGH TEMPERATURE CERAMIC SUPERCONDUCTORS (CSC) TO COMMERCIAL TOKAMAK REACTORS

D. A. Ehst
S. Kim
Y. Gohar
L. Turner
D. L. Smith
R. Mattas

October, 1987

Work supported by

Office of Fusion Energy
U.S. Department of Energy
Under Contract W-31-109-ENG-38

CONTENTS

LIST OF FIGURES

LIST OF TABLES

APPLICATION OF HIGH TEMPERATURE CERAMIC SUPERCONDUCTORS (CSC) TO COMMERCIAL TOKAMAK REACTORS

D. A. Ehst, S. Kim, Y. Gohar, L. Turner, D. L. Smith, and R. Mattas
Fusion Power Program, Argonne National Laboratory
Argonne, Illinois

ABSTRACT

Ceramic superconductors operating near liquid nitrogen temperature may experience higher heating rates without losing stability, compared to conventional superconductors. This will permit cable design with less stabilizer, reducing fabrication costs for large fusion magnets. Magnet performance is studied for different operating current densities in the superconductor, and cost benefits to commercial tokamak reactors are estimated. It appears that 10 kA · cm^{-2} (at 77 K and ~ 10 T) is a target current density which must be achieved in order for the ceramic superconductors to compete with conventional materials. At current densities around 50 kA · cm^{-2} most potential benefits have already been gained, as magnet structural steel begins to dominate the cost at this point. For a steady state reactor reductions of ~ 7% are forecast for the overall capital cost of the power plant in the best case. An additional ~ 3% cost saving is possible for pulsed tokamaks.

APPLICATION OF HIGH TEMPERATURE CERAMIC SUPERCONDUCTORS (CSC) TO COMMERCIAL TOKAMAK REACTORS

D. A. Ehst, S. Kim, Y. Gohar, L. Turner, D. L. Smith, and R. Mattas
Fusion Power Program, Argonne National Laboratory
Argonne, Illinois

1. INTRODUCTION

The recent discoveries of high temperature (~ 90K) and high field superconductivity in a class of copper oxide ceramics has stimulated a flurry of activity to assess the potential applications of these ceramic superconductors (CSC). The present report documents an initial study of the benefits that CSC materials could provide to a tokamak fusion reactor similar to STARFIRE [1]. The emphasis will be on high temperature operation, rather than high field capability, and the basic tokamak parameters will retain their STARFIRE values. Thus, the reactor size (major radius R_o = 7 m), geometry, neutron wall load (W_n = 3.7 MW/m^2) and field on axis (B_o = 5.8 T) are taken to be unaffected by the use of a CSC.

The subsystems which can benefit from using the new materials are the toroidal field coils (TFC), the inboard nuclear shield, the equilibrium field coils (EFC), and the cryoplant. These subsystems constitute 17% of the direct capital cost of the STARFIRE reactor and hence represent a substantial investment. We will show that under favorable circumstances we can expect the CSC materials to result in net cost reductions of ~ 7-8% overall. While this may not appear to be an overwhelming advance in the economic outlook for magnetic fusion, it is nevertheless an important improvement. For comparison, it was estimated [1] that steady state operation of STARFIRE resulted in a 15-20% reduction in the cost of energy (compared to pulsed operation). As with steady state operation, the use of the CSC will provide less tangible benefits which cannot be quantified. These benefits arise from magnets which are safer, more reliable, needing less inspection and maintenance, and which generally are closer to reality than the original STARFIRE design with liquid helium refrigeration.

2. MATERIALS PROPERTIES

2.1 CSC Properties

A review of the literature since December 1986 shows a large variability in the behavior of the CSC materials, which reflects the early stage of development in this field and the wide variety of compounds under study. The CSC are type II superconductors which exhibit an upper bound to current density, j_c, which varies with temperature, T, and external magnetic field. A knowledge of the j_c (T, B) surface is needed in order to design magnets in practice, but at present only a few limiting cases have been published. Thus, the B limit is very high (~ 100 T) at low T ($\lesssim$ 4K) and low j_c; whereas the T limit is large (~ 90K) when B is low (< 1T) and j_c is small. Adequately high j_c (~ 10^3 kA/cm^2) has been reported at 77 K, albeit at low B, in small samples with significant anisotropy.

Ceramics are notoriously brittle, so extreme care is necessary to fabricate practical conductors which suffer minimal breakage of the CSC components. Thus the expected mechanical properties of elastic modulus ~ 150 GPa, compressive strength ~ 150 MPa, and flexural strength ~ 60 MPa must be factored into the conductor design and matched to the mechanical properties of the stabilizer and structure in the cable. Dimensional changes and thermal and magnetic forces imposed during magnet cool down and pulsed operation must be considered. Based on our preliminary study, we recommend CSC strain limits of ~ 0.03% in flexure and ~ 0.10% in tension. The stringent flexure limit forces us to consider very thin CSC elements. Thus, if the CSC cable is wound onto a TFC with a few meters radius of curvature, the CSC filament or coating dimension should be less than ~ 1 mm. Thermal stresses can be minimized by using stabilizer and structural material with similar thermal expansion coefficients to the CSC. Quality control during conductor fabrication can minimize production of surface flaws which tend to initiate ceramic fractures. Also, winding magnets in compression will be desirable, in order to benefit from the relatively high compressive stress/strain limit.

The critical current density j_c apparently is unaffected by strain up to the point of fracture, so fracture will dictate the stress limits. For our present purposes, then, we will assume a very simplified model for the properties of the CSC. We assume that cable can be manufactured to the

requisite strain tolerances which will simultaneously operate under the following conditions:

a. Operation at T = 77 K (pool boiling, liquid nitrogen).
b. External fields B $\leq$ 10 T (STARFIRE conditions).
c. Actual current density in the CSC filaments or coatings of j_{op} = 2, 10, 50 kA/cm^2.

We consider three values of j_{op} in order to identify a goal in the development program for these new materials. By way of comparison, the STARFIRE design employed graded superconductors in the TFC, with j_{op} = 7 kA/cm^2 in the Nb_3Sn (11 T field) and j_{op} = 20, 40, 90 kA/cm^2 in the NbTi (9, 7, 5 T fields, respectively).

Radiation damage to the CSC is an area of particular concern for fusion applications, but for which we have presently very little data. Experiments have achieved neutron fluences of 2 $\times$ 10^{17} cm^{-2} (14 MeV) at room temperature on RTNS and 8 $\times$ 10^{17} cm^{-2} at IPNS, also at room temperature. A fission spectrum fluence of ~ 10^{18} cm^{-2} was achieved in Europe (KfK-Karlsruhe). No analysis of these experiments is available. As with conventional superconductors we expect the CSC properties to slightly improve at first, at low fluence, and then to deteriorate beyond a certain point. Since the CSC behavior is critically dependent upon the oxygen - copper stoichiometry we expect oxygen vacancies formed by radiation damage to be the principal concern. Conservatively, we might expect the CSC to be as robust as Nb_3Sn, which should withstand a neutron fluence of ~ 10^{19} cm^{-2} or 0.005 dpa. However, the CSC appears to tolerate a larger number of defects than Nb_3Sn and appears to have a shorter coherence length within individual crystal grains. Simple modelling encourages us to hope for roughly an order of magnitude higher resistance to radiation effects than Nb_3Sn, so for this study we postulate an additional operating condition for our CSC:

d. Neutron fluence $\leq$ 2 $\times$ 10^{20} cm^{-2} or $\leq$ 0.1 dpa.

2.2 Other Magnet Materials

Conventional superconductors require normal conducting stabilizers in parallel. Although aluminum is occasionally used, we will consider only

copper for this function. Since the stabilizer is a significant fraction of a conventional superconductor we seek to minimize its volume in the magnet, which is in part determined by its electrical resistivity. At 77 K we find any copper with RRR > 100 has essentially the same intrinsic resistivity: ρ_T = 0.2 μΩ - cm. At B = 11 T the magnetoresistivity is small: ρ_B < 0.05 μΩ - cm. Radiation-induced resistivity [2] in Cu saturates above ~ 10^{-3} dpa, and we assume this saturated value: ρ_r = 0.3 μΩ - cm. For conservation we add a safety factor and specify a total resistivity

$$\rho_{Cu} = 0.65\ \mu\Omega - cm > \rho_T + \rho_B + \rho_r \ .$$

Although an epoxy (G10) insulator was specified in the STARFIRE magnet design, it is functional only up to a radiation dose of ~ 10^9 rads. In order to operate at relatively higher neutron fluence (less inboard shielding) in the TFC we assume that ceramic insulators can be employed along with the CSC. Such insulators should survive a radiation dose ~ 10^{13} rads.

Structural materials considered for magnets are the standard austenitic stainless steels. It is unclear whether higher T operation will increase or decrease the amount and cost of steel required to withstand the tremendous magnetic forces in large magnets. Based on limited data at cryogenic temperatures [3], for a variety of alloys, we can note the following. Most steels lose strength as temperature increases. If we define S_m as the lesser of one-third the ultimate or two-thirds the yield stress, we find modest decreases in S_m between 4 K and 77 K (typically 10-30% decrease, but data is scattered with large variability). For applications to pulsed magnets (such as an ohmic heating transformer), however, cyclic stress is a more stringent constraint. Fatigue life is longer at higher T for 304LN at large strain amplitude ($\gtrsim$ 1%), but for the small strain variations ($\lesssim$ 0.5%) needed to achieve interesting life times (>10^4 cycles), the lower temperatures give superior performance. Fatigue crack growth rate studies also show large variability, and most annealed alloys (304L, 304N, 304LN, etc.) display little difference in behavior between 4 K and 77 K. We see that structural steel cost savings or increases associated with the switch from He-cooled to N_2-cooled operation are sensitive to details of the magnet designs and operating modes, which we cannot adequately address at present. In view of the uncertainties and fairly

small changes in structural properties between 4 K and 77 K, we will basically assume the structural requirements are unchanged for STARFIRE in going to the higher temperature magnets.

3. CABLE DESIGN

An important economic issue is whether the superconducting cable must be cryostable. Figure 1 shows the heat transfer coefficient to liquid N_2 from the stabilizer/CSC composite. Full cryostability demands that the coolant can carry away all heat being generated whenever the stabilizer is carrying the conductor current, and, to be conservative, the minimum Q = 0.5 W/cm^2, which occurs at ΔT = 28 K, would be specified. In practice, however, it is not necessary to be so conservative, and considerable cost reductions result (less stabilizer cross section is needed) if a larger Q is assumed. We take Q = 10 W/cm^2, at ΔT = 10 K, which is still well below the peak value (15 W/cm^2 at ΔT = 12 K) shown in Fig. 1. Such a large ΔT = 10 K would require an energy disturbance of 18 J/cm^3. It is nearly impossible to predict the magnitude of energy disturbances expected in magnets, which are due to wire movement and frictional heating, for example, but we feel confident that this is a credible upper limit. Note that a $\Delta T \leq 10$ K still keeps the CSC below 87 K, and the CSC will stay below its critical temperature and quickly recover. Such large energy inputs would not be permissible at 4 K, in contrast, because the heat capacity of materials like copper is two orders of magnitude lower at liquid He temperatures.

We considered the design of wire-geometry cables in some detail. For comparison with STARFIRE we designed a 24 kA cable composed of sixteen Rutherford sub-cables wound in parallel; see Fig. 2. Each sub-cable has six CSC/Cu composite wires wound around a steel wire for additional support.

The basic composite wire is a matrix of many CSC filaments immersed in Cu stabilizer. Dynamic stability to flux jumps places an upper limit to the filament diameter [4], d_f:

$$d_f \leq \left[8 \frac{K_{CSC}}{\rho_{Cu}} \Delta T_o R_{CS} \right]^{1/2} (J_{op})^{-1}$$

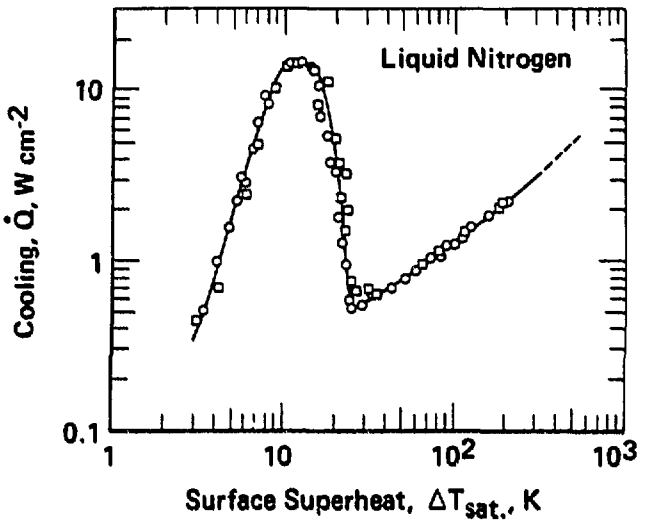

Figure 1 -- Heat transfer to liquid nitrogen.

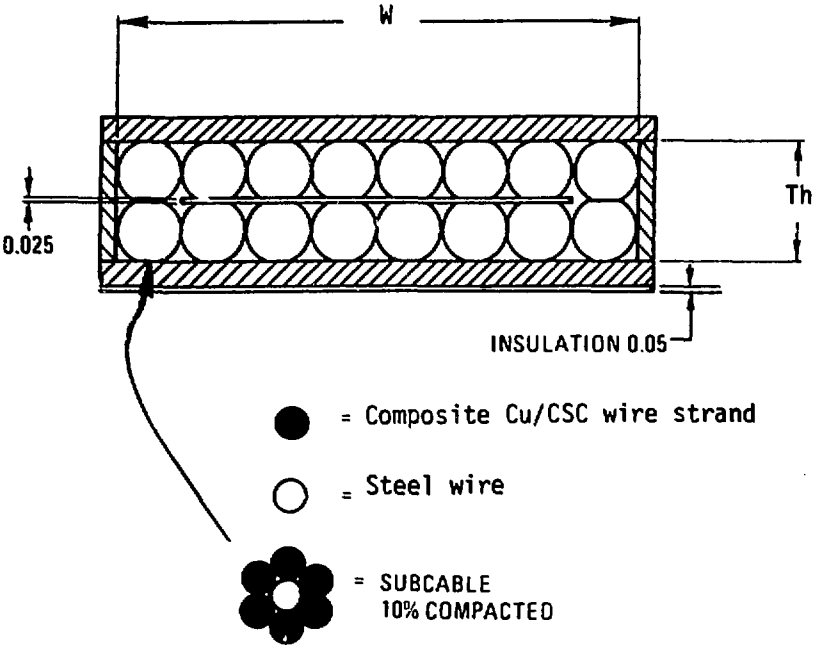

Figure 2 -- Wire based cable detail.

where K_{CSC} is the thermal conductivity of the CSC (assumed here to be 1.5×10^{-3} W cm^{-1} K^{-1}), $R_{CS} = a_{Cu}/a_{CSC}$ (ratio of stabilizer to CSC cross section in the filament), and ΔT_o is conservatively set at 13 K. For values of interest to us, $R_{CS} \approx 1$ and $j_{op} \approx 10$ kA cm^{-2}, we find $d_f \lesssim 230$ μm, which should be easily achieved.

Stekly's cryostability criterion is, per unit length of wire,

$$\frac{I^2 \rho_{Cu}}{a_{Cu}} < pQ \quad .$$

Each wire carries $I = 24 \text{ kA}/(16 \times 6) = 0.25 \text{ kA} = j_{op}\, a_{CSC}$. The wetted wire perimeter is $p = f\pi d$, where d is the wire diameter and f is the fraction in contact with N_2 (assumed to be 0.75). Combining these relations we find the minimum Cu fraction or maximum wire diameter, respectively,

$$R_{CS}^2 \,(1 + R_{CS}) \geq \frac{(\rho_{Cu}\, j_{op}^{\,2})^2}{4\pi (fQ)^2}\, a_{CSC}$$

and

$$d \leq \frac{4(fQ)\, R_{CS}(1 + R_{CS})}{j_{op}^2\, \rho_{Cu}} \quad .$$

The latter criterion is generally satisfied when the former is achieved. For the three values, $j_{op} = 2$, 10, and 50 kA cm^{-2} we have respectively $a_{CSC} = 0.125$, 0.025, and 0.005 cm^2, with $R_{CS} \geq 0.034$, 0.34, and 2.36.

The small values of R_{CS} at $j_{op} \leq 10$ kA cm^{-2} are due to the large Q available with N_2 coolant. It may not be practical to fabricate composite wire with $R_{CS} \ll 1$, so we assume a minimum value of $R_{CS} = 0.5$ in our designs. Table I summarizes the wire-based cable design for three values of j_{op}. The quantity λ_j is the cable current density averaged over the space inside the steel structural encasement. For comparison (see Table II), in STARFIRE λ_j varied from 1.7 kA cm^{-2} in the high field region to 3.45 kA cm^{-2}

in the low field region. The table indicates that j_{op} = 2 kA cm^{-2} results in a much lower λ_j than for STARFIRE, whereas j_{op} = 50 kA cm^{-2} is significantly higher. The improvement in λ_j with CSC at j_{op} = 50 kA cm^{-2} is related directly to the decreased value of R_{CS} required with N_2 cooling. [For simplicity, in our cost analysis we will not include the R_{CS} = 0.5 design at j_{op} = 10 kA cm^{-2}.]

TABLE I
WIRE CABLE DESIGN

J_{op} (kA/cm^2)	2.0	10.0		50.0
Minimum R_{CS}	0.034	0.34		2.36
R_{CS}	0.5	0.5	1.0	3.0
Strand diameter (cm)	0.49	0.22	0.25	0.16
1.5 kA - subcable diameter (cm)	1.32	0.590	0.681	0.431
Th (cm)	2.40	1.087	1.25	0.801
W (cm)	10.56	4.72	5.45	3.45
$\lambda j = \frac{24\ kA}{W \times Th}$ $(\frac{kA}{cm^2})$	0.95	4.68	3.52	8.69

TABLE II
STARFIRE COIL

B, T	11.0	9.0	7.0	5.0
n (number of turns)	180	130	128	268
R_{CS}	1.72	4.44	7.16	15.3
$n(a_{Cu} + a_{SC})$, cm^2	1597.0	883.0	610.0	1136.0
j_{op}, kA cm^{-2}	7.4	19.3	41.1	92.3
λ_j, kA cm^{-2}	1.7	2.2	3.1	3.5

Note: λ_j does not include steel structure.

An optional cable geometry was also studied. This assumed the 24 kA is built with sixteen subunits in parallel, each subunit being a thin tape or ribbon in which CSC, Cu, and insulator are laminated. Each subunit has a thickness b and width a such that the wetted perimeter is

$$p = f2a = \frac{f2a_{CSC}\,(1 + R_{CS})}{b} \quad ,$$

and cryostability now requires

$$\frac{\rho_{Cu}\, j_{op}^2\, b}{2fQ} < R_{CS}\,(1 + R_{CS}) \quad .$$

Table III gives tape-configured cable parameters for the three j_{op} values. For the selected R_{CS} values rather large b_{max} are permitted; however, should be somewhat thinner to avoid flexural stress as the cable is wound onto magnets. The λ_j is comparable for both wire- and tape-configured cables, and we thus only consider the wire geometry in the cost study which follows.

TABLE III
1.5 kA TAPE CONDUCTOR

J_{op} (kA/cm^2)	2.0	10.0		50.0	
R_{CS}	0.5	0.5	1.0	5.0	4.0
b_{max} (cm)	4.3	0.173	0.46	0.275	0.138
Chosen b (cm)	0.25	0.15	0.20	0.20	0.15
a (cm)	4.5	1.5	1.5	0.9	1.0
λ_j (kA/cm^2)	0.95	4.0	3.33	5.55	6.0

(0.1 cm - thick insulator/cooling channel is included)

4. DIRECT COST ALGORITHMS

We endeavor to compare the capital cost of the STARFIRE reactor with conventional or CSC materials. Table IV summarizes the materials costs. The unit costs are in 1983 dollars and are based on a generalization of the STARFIRE costing which was carried out in the ANL tokamak burn cycle study [5]. This costing basis includes all fabrication costs in the unit cost. Thus, for example, a steel N_2 cryostat has similar quality control requirements to a vacuum tank, but a steel He cryostat (as in the original STARFIRE design) has more stringent production standards and is thus more expensive.

For our reference comparison case we assume that the CSC unit cost will be the same as for Nb_3Sn, a similarly brittle material. Bear in mind that the TFC component costs in Table IV are much less than envisioned for near-term applications; these prices reflect large cost reductions assumed to accompany the tenth commercial STARFIRE-class reactor sometime in the next century. The cost structure reflects assumed learning-curve experience and is in accord with the STARFIRE cost structure.

5. STEADY STATE TOKAMAK - STARFIRE

5.1 Inboard Shield

Table V shows the allowed decrease in the shield if higher radiation dose is permitted in the TFC. Although ceramic insulators may tolerate very high dose rates (10^{13} rads), the CSC will no doubt be more sensitive. Assuming that the 0.1 dpa in Cu stabilizer, at 91 cm shield thickness, results in similar atomic displacements in the CSC, we cannot reduce the shield below this thickness. This shielding reduction, however, can be completely taken out of the high cost tungsten component of the shield. Relative to STARFIRE, which had 37.5 cm of W, a reduction of 29 cm is possible, leading to only 8.5 cm of W shielding. This is a mass reduction of ~ 650 Mg and a cost savings of ~ $40 M.

TABLE IV
DIRECT COST ALGORITHMS (1983 Dollars)

- Superconductor cable -- long term cost basis (burn cycle study), normalized to STARFIRE

Material	Unit Cost ($/kg)
NbTi	120
Nb_3Sn	230
CSC	230 (key assumption)
Cu	34
steel (cable, bands)	17

- Insulation --

Material	Unit Cost ($/kg)
G10	24
ceramic	30

- Cryostat -- steel cryogen container, assumed more expensive for He than N_2

Vessel	Unit Cost ($/kg)
He	31
N_2	24

- Vacuum tank -- $24/kg
- Inboard shield -- W @ $60/kg

TABLE V
CHANGE IN THE STARFIRE INBOARD SHIELD THICKNESS FOR NEW SUPERCONDUCTOR

Parameter	STARFIRE		
Inboard thickness from first wall to point of maximum field (cm)	120	91	68
Nuclear heating in superconductor winding pack (mW/cm^3)	0.0154	2.6	84
Electrical insulator dose (rads)	1.22×10^9	2.4×10^{11}	10^{13}
Fast neutron fluence (n/cm^2)	1.87×10^{17}	3.7×10^{19}	9.9×10^{20}
dpa (for Cu)	5.36×10^{-4}	0.1	4

Two assumptions are considered here:
a. The magnet is designed based on the copper saturation resistance with respect to radiation damage.
b. The insulator material functions up to 2.4×10^{11} rads.

5.2 TFC

A number of changes result in the TFC if the CSC is adopted:

1. The thinner shield allows the inboard TFC to move closer to the plasma, resulting in a lower peak field at the winding, 10.1 T.

2. The same change results in a slightly shorter perimeter for a TFC, including a somewhat lower height. Field ripple is unchanged, but the TFC stored energy decreases.

3. At the higher j_{op} values the TFC cross section is smaller than for STARFIRE, resulting in less massive, less expensive coils.

The TFC parameters for the three j_{op} values are compared with STARFIRE in Table VI. It is noteworthy that the TFC mass and cost are larger at j_{op} = 2 kA cm^{-2} than for the STARFIRE design. At j_{op} = 10 kA cm^{-2} the CSC provides a design nearly competitive with STARFIRE, while at j_{op} = 50 kA cm^{-2} the CSC is clearly superior to STARFIRE. Further increases in j_{op} are unlikely to bring substantial further cost reductions, as the steel structural requirements begin to dominate the TFC cost at large j_{op}.

In addition to potential cost reductions, the TFC operation at nitrogen temperatures will result in better mechanical support against magnetic forces. This derives from the potential use of thermal insulating supports between the room temperature vacuum tanks and the cold dewar. The STARFIRE TFC design employed G10 struts to hang the He vessel within the outboard TFC vacuum tanks, but thermal conduction limited the number and cross section of these supports. At 77 K, however, heat leakage is a smaller concern so double the number of supports may be incorporated without adversely affecting the cryoplant.

5.3 EFC

There is a secondary cost benefit to the equilibrium coil subsystem derived from improvements in the TFC system at the high j_{op} values with the CSC. Thus, at large j_{op} the radial build of the TFC is reduced by ~ 50 cm relative to the STARFIRE design, and this permits the placement of individual EF coils so much closer to the plasma. Previous study has shown [6] the EFC stored energy increases exponentially with distance from the plasma. Table VII displays the decrease in EFC energy as j_{op} increases for the CSC.

TABLE VI
COMPARISON OF TFC STRUCTURE AND COST[1]

	STARFIRE	Superconductor Type 2 kA/cm^2	10 kA/cm^2	50 kA/cm^2
B_{max} (T)	11.0	10.1	10.1	10.1
Coil length (m)	40.4	39.8	37.2	36.7
TFC energy (GJ)	50.0	48.0	41.0	39.0
TFC mass (Mg), including cryostat, vactank	5265.0	7629.0	4184.0	3461.0
Cost summary ($M)				
Nb_3Sn	11.9	---	---	---
NbTi	6.7	---	---	---
CSC[2]	---	536.3	106.0	20.8
Cu	58.8	59.0	22.1	13.1
co-wounded steel[3]	38.7	38.2	35.7	35.2
cryo vessel[4]	33.1	30.5	21.4	19.8
vacuum tank[4]	28.7	27.3	27.4	28.6
Total (incl. insulation)	179.5	693.3	214.5	119.4

[1] 1983 dollars.
[2] Ag diffusion barrier would add ~ $2M to cost of CSC.
[3] Same hoop stress in all designs.
[4] Outboard TFC designed to STARFIRE stiffness against bending.

TABLE VII
POLOIDAL COIL SYSTEM

	STARFIRE (NbTi)	Superconductor Type 2 kA/cm^2 (TF&PF)	10 kA/cm^2 (TF&PF)	50 kA/cm^2 (TF&PF)
Poloidal coil energy (GJ)	10.0	12.6	8.1	7.5
PF coil mass (Mg)	1844.0	2962.0	1801.0	1550.0
PFC cost ($M)				
NbTi	3.9	---	---	---
CSC	---	219.5	41.9	9.6
Cu	15.5	22.8	9.0	5.1
Balance	33.4	29.2	29.2	29.2
Total	52.8	271.5	80.1	43.9

The direct cost reduction in the EFC system derives from the higher average current density available for $j_{op} \geq 10$ kA cm^{-2}. The table shows comparable coil mass to STARFIRE at $j_{op} = 10$ kA cm^{-2}, but the savings in Cu stabilizer is offset by the large amount of expensive CSC needed. For this case it would be cost effective to still use inexpensive NbTi in the EFC even if the TFC employed CSC at $j_{op} = 10$ kA cm^{-2}. At the highest j_{op} there is an evident cost savings associated with the CSC. The cost savings will never be dramatic, however, because most of the EFC cost is steel structure. Elimination of the He vessel is possible, but it must be replaced with an equally massive N_2 or vacuum tank, needed to withstand the large hoop and bending forces.

5.4 Cryoplant

An obvious benefit of the CSC is that heat removal at 77 K is seven times more efficient than at 4 K, so magnets can experience higher nuclear and conduction heating without penalties in circulating electrical power. Moreover, a He refrigerator requires auxiliary components (transfer lines, liquid and gas storage) which are virtually eliminated in a nitrogen plant.

When designing superconducting coils there is a tradeoff between structural support of the cold windings and electrical power for refrigeration. Our designs with CSC employ twice the structure as in STARFIRE, giving ~ 10 kW total to the TFC. In addition, ~ 0.5 kW of heat leak is associated with current leads. The thinner shield (see Table V) results in much higher nuclear heating than in STARFIRE, with a total of ~ 80 kW of nuclear heat. Thus, as shown in Table VIII, the heat load in the CSC designs is higher than in STARFIRE, but the electrical power is almost halved. The N_2 system has an increased cost for the CSC designs relative to STARFIRE, but the He plant is nearly eliminated, resulting in large cost reductions.

5.5 Summary Cost Changes with CSC

Figure 3 displays the relative direct capital cost of STARFIRE with conventional magnets or with the high temperature CSC. The cost of STARFIRE is normalized to 100% in order to gauge the relative change in cost. The variable cost accounts (including a 15% contingency) constitute about 17% of the total STARFIRE cost.

TABLE VIII
CRYOGENIC PLANT SUMMARY

	STARFIRE	Superconductor Type 2 kA/cm^2	10 kA/cm^2	50 kA/cm^2
Heating at 4.2 K, kW	20	---	---	---
Heating at 77 K, kW	small	95	87	85
Electric power at RT, MW	7.0	4.8	4.4	4.2
Cost He system ($M)	16.8	---	---	---
Cost N_2 system	1.0	4.5	4.2	4.1
Total Cost	17.8	4.5	4.2	4.1

Notes: 1. Some He refrigeration will be needed for fueling, tritium.
2. Some additional cost savings from reduced building size.
3. CSC machines have better structural support, higher reliability.

It is clear that j_{op} = 2 kA cm^{-2} is insufficient to make the CSC practical for tokamak applications, even if the CSC cost is less than for conventional superconductors (Nb_3Sn, NbTi). However, at j_{op} = 10 kA cm^{-2} there is an evident advantage if the CSC is employed. There are continued cost reductions as j_{op} is increased to 50 kA cm^{-2}, but they are not dramatic. At the highest values of j_{op} the magnet costs are dominated by the steel structure, and this cost is not greatly affected by the properties of the superconductor.

An alternative measure of tokamak performance with the CSC is in terms of mass utilization. Compared to STARFIRE with 25,000 Mg mass for the reactor core, the CSC reactor at j_{op} = 50 kA cm^{-2} needs 2300 Mg less material and produces a slight (2 MW) additional amount of net electric power. This results roughly in a 9.4% increase in mass power density, to 51 kW/tonne.

6. PULSED TOKAMAK REACTOR

A pulsed tokamak reactor may be more expensive than the steady state STARFIRE, and it is worth inquiring if the CSC technology would provide benefits for this operating mode.

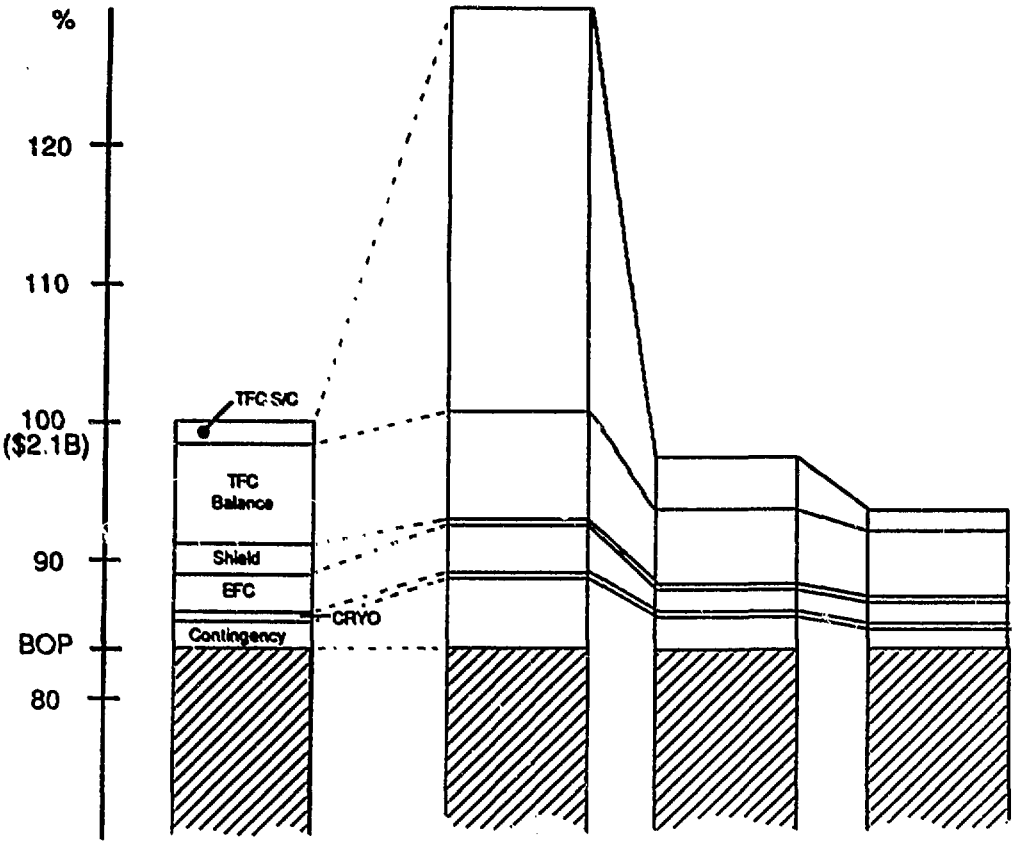

	STARFIRE	2 kA/cm2	10 kA/cm2	50 kA/cm2
Cost Reduction, reference			1.5%	6.9%
(Increase)		(26.6%)		
Cost Reduction, CSC @ $66/Kg			5.7%	7.8%
(Increase)		(5.0%)		

Figure 3
Capital cost comparison of STARFIRE with conventional and CSC magnets.

In addition to the potential cost reductions highlighted in the previous section, there are possible benefits related to longer pulse operation. Here we consider the increased volt-seconds of the transformer (OHC) if the CSC at j_{op} = 50 kA cm^{-2} is used. For this analysis we consider the design of a 10-T OHC in an 8-m major radius commercial reactor, similar to STARFIRE in electric output. This OHC, detailed in Ref. 5, provides a flux of $\Delta\phi$ = 465 V-s at a mean radius of R_{OH} = 2.72 m. The CSC increases the "hole-in-the-doughnut" to R_{OH} = 3.13 m, due to the thinner inboard shield and thinner TFC, and this increases $\Delta\phi$ by ~ 32%. For a large reactor this extends the burn time, t_f, by approximately the same fraction.

There are various benefits of extended burn time, which are related to reduced thermal and mechanical fatigue, as well as less expensive power supplies for the pulsed poloidal coils. Figure 4 shows the capital cost reductions expected for extensions of t_f [5]. Current expectations are that ohmically driven tokamaks have neoclassical resistivity, so the toroidal resistance will be a few times the Spitzer value. As the figure shows, this indicates t_f is typically about one hour, and a 32% increase in t_f represents a non-trivial (~3%) capital cost reduction for a pulsed tokamak reactor. (This is in addition to the cost reductions outlined in Section 5). Equally important, the longer burn increases the duty factor sufficiently to increase the (burn cycle averaged) net electric power by several percent.

7. ADDITIONAL BENEFITS OF THE CSC

More recent tokamak design studies [7] have pointed to the possibility that high beta stability could substantially reduce the size and cost of the TFC system. Hence, cost reductions such as shown in Fig. 3 would not be dramatic if the CSC were used. However, the new designs would have such compact TFC units that individual coils could be physically removed and replaced by overhead crane. In practice this is facilitated by mounting each coil in its own dewar, unlike the STARFIRE geometry. In order to accomplish this a robust thermal standoff must support the centering forces of the inboard winding pack against the vacuum tank. This will be an attractive application of the CSC, since the CSC can tolerate the relatively high heat leak between the warm vacuum tank and the liquid nitrogen region.

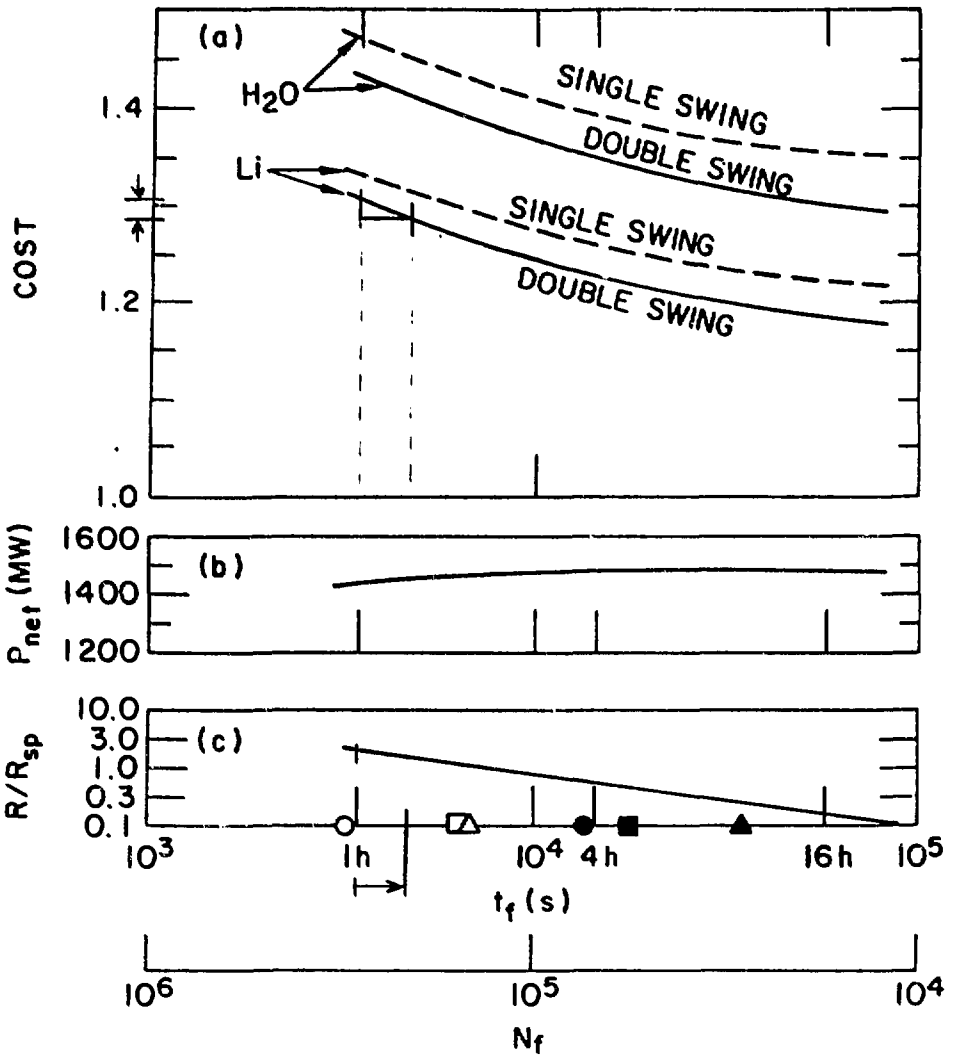

Figure 4 OH cycle; B_{OH} = 10 T, 8 m reactor. (a) Upper cost curves represent water thermal storage and near-term magnet costs, and lower curves represent liquid sodium thermal storage and long-term magnet costs. Cost is total direct capital cost normalized to STARFIRE [1]; (b) Net electric power; (c) Plasma resistance required to obtain t_f, normalized to Spitzer resistivity, R_{SP}, with Z_{eff} = 1.70, $\bar{T}_e$ = 10 KeV, and I_0 = 13.0 MA. Solid symbols are burn goals for worst case disruptions and thermal fatigue; open symbols are goals for moderate disruption damage (circles = limiter's leading edge, squares = limiter's front face, and triangles = first wall).

At low beta there are other benefits which the CSC may offer. If beta is limited to the Troyon value there is a premium on high magnetic field. For a STARFIRE-type reactor ($\beta \approx 0.06$) with maximum field at the TFC limited to $B_M \lesssim 11$ T, the electron temperature is limited ($\bar{T}_e \lesssim 18$ KeV) so current drive efficiency for steady state operation [8] is kept to a modest value, $\gamma \equiv \bar{n}_e \, I \, R_o/P_{CD} \approx 0.4$, resulting in high circulating power: $P_{CD} = 400$ MW and $Q = 6$. On the other hand, if the CSC material permitted TFC fabrication at $B_M \approx 20$ T, then the same beta could support a much higher $\bar{T}_e$, and γ and Q might be increased by over a factor of two.

Further benefits to magnetic fusion may accrue if the CSC technology is commercialized. For example, superconducting generators and transformers could play a role. Also, long distance dc power transmission lines could make remote siting of fusion power plants possible, if such an option proves desirable. Clearly there are many aspects of the CSC applications which are beyond our present study.

8. CONCLUSIONS

Several conclusions can be drawn from this preliminary assessment:

- The CSC material development program should deliver a product which carries at least 10 kA cm^{-2} at B ≈ 10 T and T = 77 K, at unit costs not much exceeding those projected for Nb_3Sn, in order to be of interest to commercial tokamaks.

- Current densities in excess of ~ 50 kA cm^{-2} are not needed.

- Flexible cable (mechanical integrity) is required.

- If the CSC survives at high radiation fluence (0.1 dpa) significant shielding savings result.

- Capital cost reductions of ~ 6-8% are foreseen for commercial tokamak reactors under the above circumstances (equivalent to several hundred million dollars for each power reactor).

- Cryogenic power, already small, is further reduced.

- Better mechanical support of cryostat is possible; separately removable TF coils.

There are equally important, but less tangible, benefits related to safety and reliability, if the CSC magnets are developed. Current leads, for example [9], have probably been responsible for more superconducting magnet failures than any other cause. Much of the mechanical weakness of leads arises from being traditionally designed to minimize the heat transfer to liquid He temperature. With N_2 operation that condition can be relaxed, and the leads can be made much stronger mechanically. Electrical arcing is another weakness of large magnets, which may be overcome with CSC, since the breakdown voltage of liquid and gaseous N_2 is far higher than for He. Most importantly, elimination of liquid He technology simplifies magnet design and introduces greater confidence that massive fusion magnets can in fact be developed in the near future.

REFERENCES

[1] C. C. Baker et al., "STARFIRE - A Commercial Tokamak Fusion Power Plant Study," Argonne National Laboratory Report, ANL/FPP-80-1 (1980).

[2] L. R. Turner and M. A. Abdou, "Computational Model for Superconducting Toroidal-Field Magnets for a Tokamak Reactor," Argonne National Laboratory Report, ANL/FPP/TM-88 (1977).

[3] "Materials Studies for Magnetic Fusion Energy Application at Low Temperatures-II," F. R. Fickett and R. P. Reed, eds., National Bureau of Standards Report, NBSIR 79-1609 (1979).

[4] M. N. Wilson et al., J. Phys. D.: Appl. Phys. 3 (1970) 1517.

[5] D. A. Ehst et al., Nucl. Eng. and Design/Fusion 2 (1985) 319.

[6] K. Evans, Jr., D. A. Ehst, and P. Messerschmidt, Proc. 3rd Top. Conf. Techn. Contr. Nucl. Fusion, CONF-780805, 2 (1978) 1084.

[7] D. Ehst et al., "Tokamak Power Systems Studies - FY 1986: A Second Stability Power Reactor," Argonne National Laboratory Report, ANL/FPP/86-1 (1987).

[8] D. A. Ehst and K. Evans, Jr., "Multiple-Wave RF Current-Driven Tokamak Reactors in the First Stability Regime," Nucl. Fusion, to be published 1987.

[9] L. R. Turner, "Safety of Superconducting Fusion Magnets: Twelve Problem Areas," Argonne National Laboratory Report, ANL/FPP/TM-121 (1979).

DISTRIBUTION FOR ANL/FPP/TM-214

Internal:

C. Baker
M. Billone
M. Brodsky
J. Brooks
Y. Cha
R. Clemmer
D. Ehst
K. Evans
P. Finn
F. Fradin
Y. Gohar
A. Hassanein
T. Hua
C. Johnson
S. Kim
A. Krauss
R. Kustom
L. LeSage
Y. Liu
S. Majumdar
R. Mattas
B. Picologlou
R. Poeppel
W. Praeg
C. Reed
J. Santiago
W. Schertz
D. Smith
M. Steindler
H. Stevens
D. Sze
L. Turner
C. Till
R. Weeks
A. Wolsky
FPP Files (20)
ANL Contract File
ANL Libraries
ANL Patent Dept.
TIS Files (5)

External:

DOE-TIC, for Distribution per UC-20d (87)
Manager, Chicago Operations Office
M. Abdou, University of California - Los Angeles
Lee Berry, Oak Ridge National Laboratory
E. Bloom, Oak Ridge National Laboratory
L. Bogart, Energy Applications & Systems, Inc.
P. Bonanos, Princeton Plasma Physics Laboratory
K. Borrass, Max Planck Institut fur Plasmaphysik, Garching
L. Bromberg, Massachusetts Institute of Technology
J. Clarke, Office of Fusion Energy
D. Cohn, Massachusetts Institute of Technology
R. Conn, University of California - Los Angeles
N. Davies, Office of Fusion Energy
S. Dean, Fusion Power Associates
V. Der, Office of Fusion Energy
R. Dowling, Office of Fusion Energy
J. File, Princeton Plasma Physics Laboratory
N. Fisch, Princeton Plasma Physics Laboratory
C. Flanagan, Oak Ridge National Laboratory
H. Forsen, Bechtel National Inc.
H. Furth, Princeton Plasma Physics Laboratory
P. Gierszewski, Canadian Fusion Fuels Technology Project
J. Gordon, TRW
G. Haas, Office of Fusion Energy
P. Haubenreich, Oak Ridge National Laboratory
C. Henning, Lawrence Livermore National Laboratory
D. Jassby, Princeton Plasma Physics Laboratory
G. Kulcinski, University of Wisconsin - Madison
R. Krakowski, Los Alamos National Laboratory
B. Logan, Lawrence Livermore National Laboratory

J. Maniscalso, TRW
T. K. Mau, University of California - Los Angeles
D. Meade, Princeton Plasma Physics Laboratory
G. Miley, University of Illinois - Champaign-Urbana
B. Montgomery, Massachusetts Institute of Technology
F. Najmabdai, University of California - Los Angeles
A. Opdenaker, Office of Fusion Energy
S. Piet, EG&G Idaho
P. Rutherford, Princeton Plasma Physics Laboratory
J. Santarius, University of Wisconsin
K. Schultz, GA Technologies Inc.
J. Schultz, Massachusetts Institute of Technology
T. Shannon, Oak Ridge National Laboratory
J. Sheffield, Oak Ridge National Laboratory
W. M. Stacey, Georgia Institute of Technology
D. Steiner, Rensselaer Polytechnic Institute
P. Stone, Office of Fusion Energy
L. Summers, Lawrence Livermore National Laboratory
K. Thomassen, Lawrence Livermore National Laboratory
P. Walstrom, University of Wisconsin
C. Weggel, Energy Application & Systems, Inc.